

Z. Q. Li,^{1,*} E. A. Henriksen,² Z. Jiang,^{2,3} Z. Hao,⁴ M. C. Martin,⁴ P. Kim,² H. L. Stormer,^{2,5,6} and D. N. Basov¹

¹*Department of Physics, University of California, San Diego, La Jolla, California 92093, USA*

²*Department of Physics, Columbia University, New York, New York 10027, USA*

³*National High Magnetic Field Laboratory, Tallahassee, Florida 32310, USA*

⁴*Advanced Light Source Division, Lawrence Berkeley National Laboratory, Berkeley, California 94720, USA*

⁵*Department of Applied Physics and Applied Mathematics, Columbia University, New York, New York 10027, USA*

⁶*Bell Labs, Alcatel-Lucent, Murray Hill, New Jersey 07974, USA*

(Dated: November 30, 2008)

We report on infrared spectroscopy of bilayer graphene integrated in gated structures. We observe a significant asymmetry in the optical conductivity upon electrostatic doping of electrons and holes. We show that this finding arises from a marked asymmetry between the valence and conduction bands, which is mainly due to the inequivalence of the two sublattices within the graphene layer and the next nearest neighbor interlayer coupling. From the conductivity data, the energy difference of the two sublattices and the interlayer coupling energy are directly determined.

Recently there has been unprecedented interest in carbon-based materials due to the discovery of graphene [1]. Among all carbon systems, bilayer graphene stands out due to its remarkable properties such as a unique quantum Hall effect stemming from a previously unknown type of quasiparticles, massive chiral quasiparticles[2]. Bilayer graphene is predicted to show strong many body interactions due to the unusual shape of the Fermi surface[3]. Moreover, it is the only known semiconductor with a tunable band gap between the valence and conduction bands [4][5] [6][7], which demonstrates its great potential for future nano-electronic applications. Therefore, it is of utmost importance to acquire a comprehensive understanding of this material. One central issue is how the Dirac quasiparticles in single layer graphene are modified when two graphene sheets are stacked together in bilayer graphene. The vast majority of previous experimental and theoretical studies have assumed that the electronic band structure of bilayer graphene is symmetric. This is in contrast with a significant electron-hole asymmetry observed in cyclotron resonance [8] and cyclotron mass experiments[4]. Several theoretical proposals have been put forward to explain these results [4][9]. However, our current understanding of the observed effects remains incomplete. Furthermore, the interlayer coupling energy γ_1 that controls the fundamental properties of bilayer graphene is yet to be determined [4][10][11].

Here we present the first investigation of the optical conductivity of bilayer graphene via infrared spectroscopy. We observed dramatic differences in the evolution of the conductivity for electron and hole polarities of the gate voltage. We show that small band parameters other than γ_1 give rise to an asymmetry between the valence and conduction bands [10], in contrast to the commonly assumed symmetric band structure. The systematic character of our IR data enables us to extract an energy difference between the A and B sublattices within

the same graphene layer (Fig 1(b)) of $\delta_{AB} \approx 18\text{meV}$. Moreover, the value of γ_1 , $\approx 404\text{meV}$, is determined from direct measurements of interband transitions. We discuss the broad implications of these findings for the fundamental understanding of bilayer graphene.

Infrared (IR) reflectance $R(\omega)$ and transmission $T(\omega)$ measurements were performed on bilayer graphene samples on SiO_2/Si substrate [8] as a function of gate voltage V_g at 45K employing synchrotron radiation, as described in [12]. We find that both $R(\omega)$ [13, 14] and $T(\omega)$ spectra of the bilayer graphene device can be strongly modified by a gate voltage. Figure 1 shows the transmission ratio data at several voltages normalized by data at the charge neutrality voltage V_{CN} : $T(V)/T(V_{CN})$, where V_{CN} is the voltage corresponding to the minimum DC conductivity, and $V = V_g - V_{CN}$. The $T(V)/T(V_{CN})$ spectra are dominated by a dip at around 3000 cm^{-1} , the magnitude of which increases systematically with voltage. Apart from the main dip, a peak was observed in the $T(V)/T(V_{CN})$ data below 2500 cm^{-1} , which shifts systematically with voltage. This latter feature is similar to the $T(V)/T(V_{CN})$ data for single layer graphene [12]. The gate-induced enhancement in transmission ($T(V)/T(V_{CN}) > 1$) below 2500 cm^{-1} and above 3500 cm^{-1} implies a decrease of the absorption with voltage in these frequency ranges.

The most informative quantity for exploring the quasi-particle dynamics in bilayer graphene is the two dimensional (2D) optical conductivity $\sigma_1(\omega) + i\sigma_2(\omega)$ [12][15]. First, we extracted the optical conductivity at V_{CN} from the reflectance data (not shown) employing a multilayer analysis of the device [12][15]. We find that $\sigma_1(\omega, V_{CN})$ has a value of $2 * (\pi e^2/2h)$ at high energies, with a pronounced peak at 3250 cm^{-1} (inset of Fig 2(b)). This observation is in agreement with theoretical analysis on undoped bilayer graphene[16][17][18]. Our high energy data agree with recent experiments in the visible region [19]. The peak around 3250 cm^{-1} can be assigned to the

interband transition in undoped bilayer near the interlayer coupling energy γ_1 .

An applied gate voltage shifts the Fermi energy E_F to finite values leading to significant modifications of the optical conductivity. The $\sigma_1(\omega, V)$ and $\sigma_2(\omega, V)$ spectra extracted from voltage-dependent reflectance and transmission data [12] are shown in Fig 2. At frequencies below 2500 cm^{-1} , we observe a suppression of $\sigma_1(\omega, V)$ below $2\pi(\pi e^2/2h)$ and a well-defined threshold structure, the energy of which systematically increases with voltage. Significant conductivity was observed at frequencies below the threshold feature. These observations are similar to the data in single layer graphene [12]. The threshold feature below 2500 cm^{-1} can be attributed to the onset of interband transitions at $2E_F$, as shown by the arrow labeled e_1 in the inset of Fig 2(a) and (b). The observed residual conductivity below $2E_F$ is in contrast to the theoretical absorption for ideal bilayer graphene [17][18] that shows nearly zero conductivity up to $2E_F$. Similar to single layer graphene, the residual conductivity may originate from disorder effects [17] or many body interactions [12]. Apart from the above similarities, the optical conductivity of bilayer graphene is significantly different from the single layer conductivity. First, the energy range where the conductivity $\sigma_1(\omega, V)$ is impacted by the gate voltage extends well beyond the $2E_F$ threshold. Furthermore, we find a pronounced peak near 3000 cm^{-1} , the oscillator strength of which shows a strong voltage dependence. This peak originates from the interband transition between the two conduction bands or two valence bands (inset of Fig.2a) [17][18].

The voltage dependence of the Fermi energy in bilayer graphene can be extracted from $\sigma_2(\omega, V)$ using a similar procedure as in [12]. In order to isolate the $2E_F$ feature, we fit the main resonance near 3000 cm^{-1} with Lorentzian oscillators and then subtracted them from the experimental $\sigma_2(\omega, V)$ spectra to obtain $\sigma_2^{diff}(\omega, V)$. The latter spectra reveal a sharp minimum at $\omega=2E_F$ (Fig 2(c)) in agreement with single layer graphene [12]. Figure 3a depicts the experimental $2E_F$ values along with the theoretical result in [7]. Assuming the Fermi velocity v_F in bilayer graphene is similar to that in single layer graphene ($v_F=1.1 \times 10^6 \text{ m/s}$), we find that our data can be fitted with $\gamma_1=450 \pm 80 \text{ meV}$. Equally successful fits can be obtained assuming the Fermi velocity and interlayer coupling in the following parameter space: $v_F=1.0-1.1 \times 10^6 \text{ m/s}$ and $\gamma_1=360-450 \text{ meV}$. Previous studies showed that an applied gate voltage opens a gap Δ between the valence and conduction bands [4][5][6][7]. Because $\Delta(V)$ is much smaller than $2E_F(V)$ for any applied bias in bottom-gate devices [7], it has negligible effects on the experimentally observed $2E_F(V)$ behavior.

The central result of our study is an observation of a pronounced asymmetry in evolution of the optical conductivity upon injection of electrons or holes in bilayer

graphene. Specifically, the frequencies of the main peak ω_{peak} in $\sigma_1(\omega, V)$ are very distinct for E_F on the electron and hole sides, as shown in Fig 3(b). In addition, ω_{peak} on the electron side shows a much stronger voltage dependence compared to that on the hole side. All these features are evident in the raw data in Fig.1, where the resonance leads to a dip in $T(V)/T(V_{CN})$ spectra. These behaviors are reproducible in multiple gated samples. Such an electron-hole asymmetry is beyond a simple band structure only taking γ_1 into account, which predicts symmetric properties between electron and hole sides.

The electron-hole asymmetry in our $\sigma_1(\omega, V)$ data can be explained by an asymmetry between valence and conduction bands [20]. Such an asymmetric band structure arises from finite band parameters δ_{AB} and v_4 , where δ_{AB} (denoted as Δ in [21][17]) is the energy difference between A and B sublattices within the same graphene layer, and $v_4=\gamma_4/\gamma_0$. γ_4 and γ_0 are defined as interlayer next-nearest-neighbor coupling energy and in-plane nearest-neighbor coupling energy, respectively [21][17]. We first illustrate the effects of δ_{AB} and v_4 on the energy bands of bilayer graphene $E_i(\mathbf{k})$ ($i=1,2,3,4$), which can be obtained from solving the tight binding Hamiltonian Eq (6) in Ref. [17]. It is evident that finite values of δ_{AB} and v_4 break the symmetry between valence and conduction bands, as schematically shown in the inset of Fig 2(a). Specifically, δ_{AB} induces an asymmetry in E_1 and E_4 bands such that $E_1 > -E_4$ at $\mathbf{k}=0$, whereas v_4 induces an electron-hole asymmetry in the slope of the valence and conduction bands. With finite v_4 , the bands E_1 and E_2 are closer and E_3 and E_4 are further apart at high \mathbf{k} compared to those with zero v_4 value.

Next we examine the effects of δ_{AB} and v_4 on $\sigma_1(\omega, V)$. It was predicted theoretically [18] that the main peak in $\sigma_1(\omega, V)$ occurs in the frequency range between two transitions labeled e_2 and e_3 as shown in the inset of Fig 2(a) and (b). Here $e_2=-E_4(\mathbf{k}=0)-\Delta/2$ and $e_3=E_3(\mathbf{k}=k_F)-E_4(\mathbf{k}=k_F)$ for the hole side, and $e_2=E_1(\mathbf{k}=0)-\Delta/2$ and $e_3=E_1(\mathbf{k}=k_F)-E_2(\mathbf{k}=k_F)$ for the electron side[18], with Δ defined as the gap at $\mathbf{k}=0$. For zero values of δ_{AB} and v_4 , e_2 and e_3 transitions are identical on the electron and hole sides. The finite values of δ_{AB} and v_4 induce a significant inequality between e_2 and e_3 on the electron and hole sides. We first focus on the low voltage regime, where $\omega_{peak}=e_2=e_3$. Because v_F and v_4 always enter the Hamiltonian in the form of $v_F k$ and $v_4 k$ products[17], these terms give vanishing contributions at low V , where \mathbf{k} goes to zero. Consequently, ω_{peak} value at low bias is solely determined by γ_1 and δ_{AB} , with $\omega_{peak}=\gamma_1 + \delta_{AB}$ and $\omega_{peak}=\gamma_1 - \delta_{AB}$ for the electron and hole sides, respectively. At V_{CN} (0V), interband transitions between the two conduction bands and the two valence bands are both allowed, which leads to a broad peak centered between $\gamma_1 + \delta_{AB}$ and $\gamma_1 - \delta_{AB}$ (Fig 3(b)). From the two distinct low voltage ω_{peak} val-

ues on the electron and hole sides shown in Fig 3(b), the values of γ_1 and δ_{AB} can be determined with great accuracy: $\gamma_1=404\pm 10\text{meV}$ and $\delta_{AB}=18\pm 2\text{meV}$. Therefore, the $\sigma_1(\omega, V)$ data at low biases clearly indicates an asymmetry between valence and conduction bands in bilayer graphene due to finite energy difference of A and B sublattices.

In order to explore the V dependence of ω_{peak} , we plot the e_2 and e_3 transition energies [18] as a function of V (Fig. 3b), using the gap formula $\Delta(V)$ in [7][22] and our calculated asymmetric dispersion $E_i(k)$ ($i=1,2,3,4$) [23], with $v_F=1.1\times 10^6\text{m/s}$, $\gamma_1=404\text{meV}$, $\delta_{AB}=18\text{meV}$, and for both $v_4 = 0$ and $v_4 = 0.04$. We find that e_2 does not depend on v_4 [22], whereas e_3 is strongly affected by v_4 . With a finite value of v_4 (≈ 0.04), an assignment of ω_{peak} to $(e_2+e_3)/2$ appears to fit our data well on both electron and hole sides. The finite value of the v_4 parameter [10] is essential to qualitatively account for the voltage dependence of ω_{peak} , because with $v_4\approx 0$, ω_{peak} follows e_2 and e_3 on the electron and hole sides (Fig 3b), respectively, eluding a consistent description. Recently, a systematic theoretical analysis of the V dependence of ω_{peak} and the lineshape of the conductivity spectra has been reported in ref. [20]. It is found that the infrared data presented here are consistent with a v_4 value of ≈ 0.05 [20].

We stress that γ_1 and δ_{AB} are determined from the low bias (low k_F) data. Therefore the values of γ_1 and δ_{AB} reported here do not suffer from the currently incomplete understanding of the infrared data at high biases [20]. The γ_1 value ($404\pm 10\text{meV}$) is directly determined from measurements of transitions between the two conduction bands or valence bands without any assumptions. This value is more accurate than previous indirect measurements of γ_1 [4][10][11]. The accurate determination of γ_1 is paramount since it governs the fundamental properties of bilayer such as the quantitative behavior of the tunable band gap [4][7].

IR measurements reported here have enabled accurate extraction of δ_{AB} in bilayer graphene free from ambiguities of alternative experimental methods. It is interesting to compare this value with the energy difference between A and B sublattices δ_{AB} in graphite, which is about 36meV [20][21]. Note that, in graphite, $\delta_{AB} = \Delta - \gamma_2 + \gamma_5$, where γ_2 and γ_5 are interlayer coupling band parameters [20]. As pointed out in [20], $\delta_{AB}(\text{graphite}) \sim 2\delta_{AB}(\text{bilayer})$ is exactly what one would expect within the tight binding model. In the bilayer each A atom has a single stacking partner while in the Bernal graphite it has two of them, therefore, $\delta_{AB}(\text{graphite}) \sim 2\delta_{AB}(\text{bilayer})$.

The asymmetry between valence and conduction bands uncovered by our study has broad implications on the fundamental understanding of bilayer graphene. An electron-hole asymmetry was observed in the cyclotron resonance [8] and cyclotron mass experiments [4] in bi-

layer; both experiments have eluded a complete understanding so far. Our accurate determination of finite values of δ_{AB} and v_4 calls for explicit account of the asymmetric band structure in the interpretation of the cyclotron data. Moreover, the different δ_{AB} values in bilayer graphene and graphite reveal the importance of interlayer coupling in defining the electronic properties and band structure of graphitic systems.

During the preparation of this paper, we became aware of another infrared study of bilayer graphene by A.B. Kuzmenko et al [14]. We thank M. L. Zhang and M. M. Fogler for their discussions on the theoretical interpretations of the data, and A. H. Castro Neto for valuable comments on the manuscript. Work at UCSD is supported by DOE (I will provide new DOE Mon). Research at Columbia University is supported by the DOE (No. DE-AIO2-04ER46133 and No. DE-FG02-05ER46215), NSF (No. DMR-03-52738 and No. CHE-0117752), NYSTAR, the Keck Foundation and Microsoft, Project Q. The Advanced Light Source is supported by the Director, Office of Science, Office of Basic Energy Sciences, of the U.S. Department of Energy under Contract No. DE-AC02-05CH11231.

* Electronic address: zhiqiang@physics.ucsd.edu

- [1] K. S. Novoselov et al, Nature 438, 197 (2005); Y. Zhang et al, Nature 438, 201 (2005); A. K. Geim and K. S. Novoselov, Nat. Mater. 6, 183 (2007); A. K. Geim and A. H. MacDonald, Phys. Today 60, 35 (2007); A. H. Castro Neto et al, arXiv:cond-mat/0709.1163.
- [2] K. S. Novoselov et al, Nature Phys. 2, 177 (2006).
- [3] J. Nilsson et al., Phys. Rev. B 73, 214418 (2006); T. Stauber et al., Phys. Rev. B 75, 115425 (2007).
- [4] E. V. Castro et al, Phys. Rev. Lett. 99, 216802 (2007).
- [5] T. Ohta et al, Science 313, 951 (2006).
- [6] E. McCann and V. I. Fal'ko, Phys. Rev. Lett. 96, 086805 (2006); F. Guinea et al, Phys. Rev. B 73, 245426 (2006); J. Nilsson et al, Phys. Rev. B 76, 165416 (2007); H. Min et al, Phys. Rev. B 75, 155115 (2007).
- [7] E. McCann, Phys. Rev. B 74, 161403(R) (2006).
- [8] E. Henriksen et al, Phys. Rev. Lett. 100, 087403 (2008).
- [9] S. V. Kusminskiy, D. K. Campbell, A. H. Castro Neto, arXiv:cond-mat/0805.0305.
- [10] L. M. Malard et al, Phys. Rev. B 76, 201401(R) (2007).
- [11] J. Yan, E. A. Henriksen, P. Kim, and A. Pinczuk, Phys. Rev. Lett. 101, 136804 (2008).
- [12] Z.Q. Li et al, Nature Physics 4, 532 (2008).
- [13] F. Wang et al, Science 320, 206 (2008).
- [14] A.B. Kuzmenko et al, arXiv:0810.2400.
- [15] Z.Q. Li et al, Phys. Rev. Lett. 99, 016403 (2007).
- [16] J. Nilsson et al, Phys. Rev. Lett. 97, 266801 (2006); D. S. L. Abergel and V. I. Fal'ko, Phys. Rev. B 75, 155430 (2007).
- [17] J. Nilsson et al, Phys. Rev. B 78, 045405 (2008).
- [18] E. J. Nicol and J. P. Carbotte, Phys. Rev. B 77, 155409 (2008).
- [19] R.R. Nair et al, Science 320, 1308 (2008).

FIG. 1: (color online) $T(V)/T(V_{CN})$ spectra of bilayer graphene. (a) and (b): data for E_F on the hole side and electron side. Inset of (a): a schematic of the device and infrared measurements. Inset of (b): a schematic of bilayer graphene with the interlayer coupling parameters shown. The A and B sublattices are shown in different colors. The sublattice A_1 is right on top of the sublattice A_2 .

FIG. 2: (color online) The optical conductivity of bilayer graphene. (a) and (b): $\sigma_1(\omega, V)$ data for E_F on the hole side and electron side. (c): $\sigma_2^{diff}(\omega, V)$ spectra in the low frequency range, after subtracting the Lorentzian oscillators describing the main resonance around 3000 cm^{-1} from the whole $\sigma_2(\omega, V)$ spectra. Inset of (a): Schematics of the band structure of bilayer with zero values of δ_{AB} and v_4 (red) and finite values of δ_{AB} and v_4 (black), together with allowed interband transitions. Insets of (b): $\sigma_1(\omega, V)$ at $0V$ (V_{CN}) and $40V$ on the hole side with assignments of the features.

[20] L. M. Zhang et al, arXiv:0809.1898.

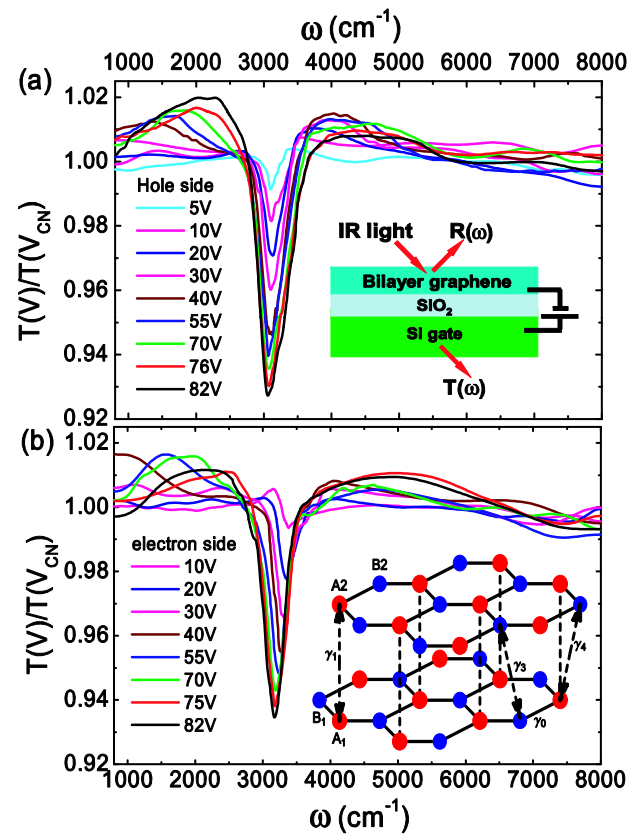
[21] N. B. Brandt, S. M. Chudinov and Ya. G. Ponomarev, *Semimetals 1: Graphite and its Compounds* (North-

Holland, Amsterdam, 1988). D. D. L. Chung, *Journal of Materials Science* 37, 1 (2002).

[22] The gap formula $\Delta(V)$ in [7] did not take into account δ_{AB} and v_4 . However, we find that finite δ_{AB} and v_4 values have negligible effect on the gap Δ . Specifically, δ_{AB} primarily modifies the E_1 and E_4 bands, while leaving unchanged the gap Δ between the E_2 and E_3 bands at $k=0$, as shown in Fig 2(a). In addition, v_4 always appears in a term v_4k in the Hamiltonian[17], therefore it has zero effect on Δ .

[23] In the calculation of the energy bands $E_i(k)$ ($i=1,2,3,4$), we used the approximation $\Delta=0$, which can be justified for the purpose of estimating e_2 and e_3 . The gap Δ is very small ($<80\text{ meV}$) in the voltage range studied in our work [7], and hardly affects the higher energy bands $E_1(k=0)$ or $E_4(k=0)$ and therefore the value of e_2 . Note that $\Delta=0$ is only assumed when calculating $E_i(k)$, but not in the Δ term in the expression of e_2 . Moreover, E_2 and E_3 bands are modified by the gap mostly at energies below $\Delta/2$. Because E_F is much larger than $\Delta/2$ under applied voltage [7], $E_2(k=k_F)$ and $E_3(k=k_F)$ are not affected by Δ . Therefore, a finite gap does not modify the value of e_3 compared to that with $\Delta=0$.

FIG. 3: (color online) (a) Symbols: the $2E_F$ values extracted from the optical conductivity detailed in the text. The error bars are estimates of the uncertainties of $\sigma_2^{diff}(\omega, V)$ spectra in Fig 2(c). Solid lines: the theoretical $2E_F$ values using $v_F=1.1 \times 10^6$ m/s and $\gamma_1=450$ meV. (b) Solid symbols, the energy of the main peak ω_{peak} in the $\sigma_1(\omega, V)$ spectrum. Open symbols: the energy of the dip feature ω_{dip} in the $T(V)/T(V_{CN})$ spectra. Note that ω_{peak} in $\sigma_1(\omega, V)$ is shifted from ω_{dip} in the raw $T(V)/T(V_{CN})$ data with an almost constant offset, which is due to the presence of the substrate. Solid lines: theoretical values of the transitions at e_2 , e_3 and $(e_2+e_3)/2$ with $v_F=1.1 \times 10^6$ m/s, $\gamma_1=404$ meV and $\delta_{AB}=18$ meV and $v_4=0.04$. Red dashed lines: e_3 with similar parameters except $v_4=0$.



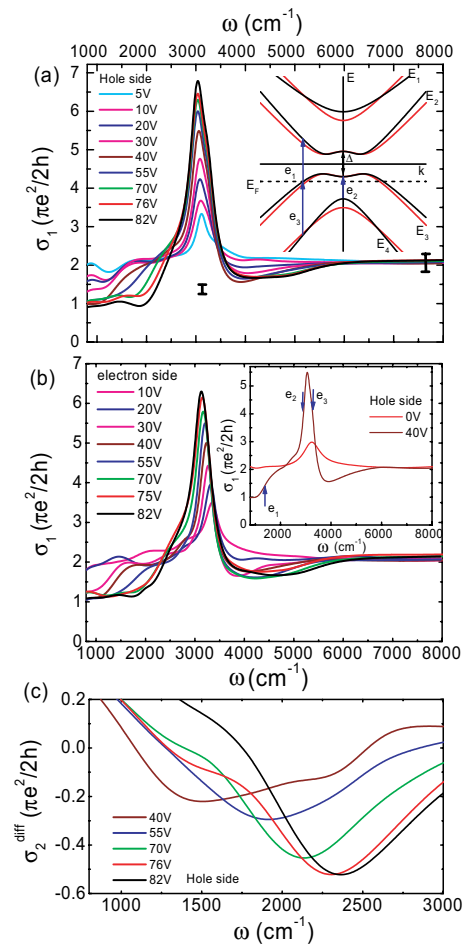


Figure 2

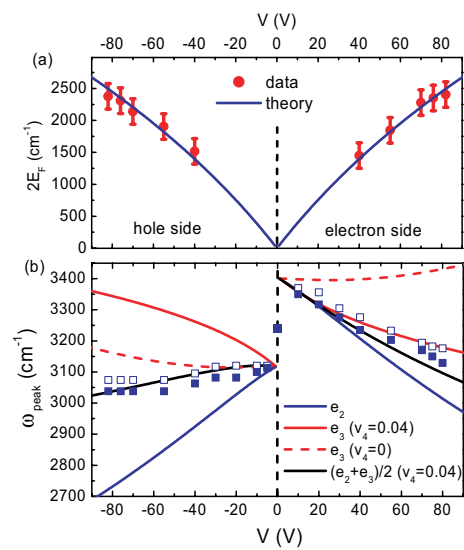


Figure 3